Journal of Coastal Research	23	3	749–763	West Palm Beach, Florida	May 2007

Assessing Effects of Data Limitations on Salinity Forecasting in Barataria Basin, Louisiana, with a Bayesian Analysis

Emad Habib[†], William K. Nuttle[‡], Victor H. Rivera-Monroy[§], Shankar Gautam[†], Jing Wang[††], Ehab Meselhe[†], and Robert R. Twilley[§]

[†]Department of Civil Engineering
University of Louisiana at Lafayette
Lafayette, LA, 70504, U.S.A.

[‡]Eco-Hydrology
11 Craig Street
Ottawa, ON K1S 4B6, Canada

[§]Department of Oceanography and Coastal Sciences
Wetland Biogeochemistry Institute
Louisiana State University
Baton Rouge, LA 70803, U.S.A.

[††]Department of Experimental Statistics
Louisiana State University
Baton Rouge, LA 70803, U.S.A.

ABSTRACT

HABIB, E.; NUTTLE, W.K.; RIVERA-MONROY, V.H.; GAUTAM, S.; WANG, J.; MESELHE, E., and TWILLEY, R.R., 2007. Assessing effects of data limitations on salinity forecasting in Barataria basin, Louisiana, with a Bayesian analysis. *Journal of Coastal Research,* 23(3), 749–763. West Palm Beach (Florida), ISSN 0749-0208.

Reliable forecasts of salinity changes are essential for restoring and sustaining natural resources of estuaries and coastal ecosystems. Because of the physical complexity of such ecosystems, information on uncertainty associated with salinity forecasts should be assessed and incorporated into management and restoration decisions. The objective of this study was to investigate uncertainty in salinity forecasts imposed by limitations on data available to calibrate and apply a mass balance salinity model in the Barataria basin, Louisiana. The basin is an estuarine wetland-dominated ecosystem located directly west of the Mississippi Delta complex. The basin has been experiencing significant losses of wetland at a rate of nearly 23 km^2/y. A Bayesian-based methodology was applied to study the effect of data-related uncertainty on both the retrieval of model parameters and the subsequent model predictions. We focused on uncertainty caused by limited sampling and coverage of salinity calibration data and by sparse rain gauge data within the basin. The results indicated that data limitations lead to significant uncertainty in the identification of model parameters, causing moderate to large systematic and random errors in model results. The most significant effect was related to lack of accurate information on rainfall, a major source of fresh water in the basin. The approach and results of this study can be used to identify necessary improvements in monitoring of complex estuarine systems that can decrease forecast uncertainty and allow managers greater accuracy in planning restoration of coastal resources.

ADDITIONAL INDEX WORDS: *Uncertainty analysis, Barataria basin, coastal Louisiana, rainfall sampling, model calibration, parametric uncertainty, salinity, restoration.*

INTRODUCTION

Ecological forecast models play a central role in restoring and sustaining natural resources of estuaries and coastal waters. Ecological forecasts provide quantitative information that managers need to evaluate risks and benefits anticipated from different ecological trajectories and their associated management scenarios (SIMENSTAD, REED, and FORD, 2006). Risk and benefit calculations might be based on ecological performance measures (THOM, 2000) or, as is likely in the wake of hurricanes Katrina and Rita, they might be based on mitigating future losses from coastal flooding (HOUCK, 2006). In any case, managers need information on the uncertainty in the forecasts so that they can judge whether the risks and benefits presented by one trajectory differ significantly from those of another trajectory. The underlying question is whether different approaches to restoring coastal resources will have significantly different results.

Uncertainty that arises in making ecological forecasts fall into the category of "knowledge uncertainty," which is one of three general categories of uncertainty that resource managers must take into consideration (ENGELUND, XU, and GOTTSCHALK, 2005; LALL *et al.,* 2002; NRC 2002; REFSGAARD and STORM, 1996). Other categories are the "inherent uncertainty" that arises from the variability of processes in nature and the "decision uncertainty" that is related to understanding management goals and the scope of activities required to achieve these goals. Ecological forecasting capabilities are limited by factors such as incomplete understanding of the processes involved, inaccuracies in model formulation, and inadequate or erroneous information needed to apply the models (*i.e.,* input and calibration data, and values of model parameters).

Salinity is an essential characteristic of estuarine and coastal ecosystems, and often, changes in salinity constitute a link in the chain of cause and effect that connects activities in upstream watersheds to ecological effects along the coast. In coastal Louisiana, the salinity of surface waters is recognized as a primary factor in the productivity of coastal fisheries (*e.g.,* TURNER, 2006) and in determining the extent and

DOI: 10.2112/06-0723.1 received 12 July 2006; accepted in revision 14 September 2006.

spatial distribution of freshwater, mesohaline, and euhaline wetland communities (VISSER *et al.,* 2000). Human activities affect estuarine salinity directly by either changing the amount or timing of freshwater inflow or altering the waterbody hydrodynamics and the rate of mixing with the coastal ocean. Therefore, resource managers must be able to predict changes in estuarine salinity that can occur as a result of activities currently proposed for restoring coastal ecosystems.

This study investigates the sources and the magnitudes of uncertainty in forecasting salinity in the Barataria basin, Louisiana. Currently, managers divert water and sediment from the Mississippi River into the adjacent wetlands and estuarine areas as a mechanism to reduce wetland loss and restore coastal habitats (DELAUNE *et al.,* 2005). The ability to forecast how this will affect the salinity, and thus the ecology, in these areas depends on the data available for input to and calibration of forecast models. In this study, we examine the influence of errors associated with estimating basin-wide rainfall (model input data) and salinity (model calibration data) in the major waterbodies within the Barataria basin. Errors in estimating these quantities arise from various sources, such as instrumental errors, missing data, and the application of spatially limited data to estimate variations in rainfall and salinity fields over basin subscales.

Operationally, we measure uncertainty as the expected deviation of a quantity from its true value. Therefore, to study the effects of uncertainty in rainfall and salinity, we must know their true values in nature, or at least assume to know them. In this setting, we define the true state of nature in the Barataria basin by time series of "true" rainfall values and by a model that represents the "true" relationship between rainfall and salinity. The relationship is defined by specifying "true" values for the model parameters. The salinity calculated by the model is considered as the "true" salinity values. A similar approach was used by RAAT *et al.* (2004) to study uncertainty in catchment nitrogen modeling.

We examine the effects of uncertainty in rainfall input data and salinity calibration data by (1) contaminating the assumed true rainfall and salinity data with error, (2) recalibrating the model to estimate the optimal values for its parameters on the basis of the contaminated data, and (3) comparing these parameter values and the corresponding predicted salinities with their "true" values. This approach is implemented with the use of an optimization and uncertainty analysis Bayesian method, which allows examination of the effects of data uncertainties on the estimation of model parameters and the subsequent salinity predictions.

Our analysis provides insights into how forecast uncertainty can be reduced through more accurate estimates of processes that drive the ecosystem change and response. Can we state whether insufficient rainfall or salinity data is the more significant source of uncertainty? Do separate effects of each variable combine additively or in a more complex way? Should we focus on developing more complex models, or do we need to improve existing data collection strategies to reduce uncertainty in representing the main driving process and estimating model parameters?

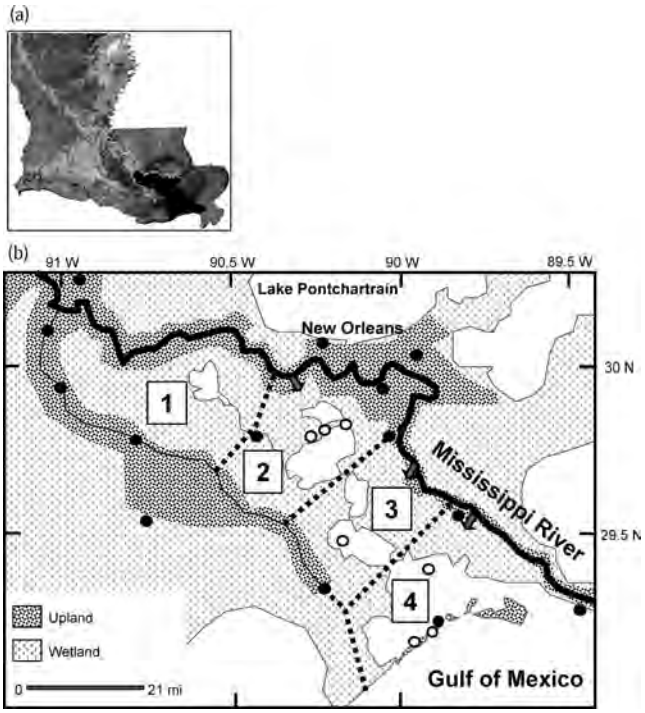

Figure 1. (a) Location map showing the location of Barataria Bay in coastal Louisiana. (b) Monitoring sites for salinity (open circles), rainfall (black circles), and sea level data used by the mass balance model. Solid arrows indicate the locations of the main river diversions: Davis Pond, Naomi, and West Pointe á la Hache (from north to south). Boundaries of the four subbasins used by the model to represent the estuary are also shown.

METHODS

Study Site

The Barataria basin is an estuarine wetland system in the Mississippi Delta in south Louisiana. The basin is located between the natural levees of the Mississippi River on the east and Bayou Lafourche on the west (Figure 1) and is separated from the Gulf of Mexico by a chain of barrier islands (FITZGERALD *et al.,* 2004). The basin encompasses a total of approximately 6000 km^2 of waterbodies and wetlands and has experienced significant losses of wetland at a rate of nearly 23 km^2/y between 1974 and 1990 (COLEMAN, ROBERT, and STONE, 1998; STONE *et al.,* 1997). This is attributed to flood control levees and continuous deepening and maintenance of navigation channels, which are starving the wetlands from seasonal inputs of fresh water and sediment from the river (BOESCH *et al.,* 1994). On the basis of the locations of major waterbodies, the basin can be divided into a series of four interconnected subbasins (Figure 2). The northern part of the basin is occupied by several large lakes, whereas the southern part consists of tidally influenced marshes connected to a large bay system behind the barrier islands (PENLAND, BOYD, and SUTTER, 1988).

With the Mississippi River constrained within its main channel by levees since the first half of the 20th century,

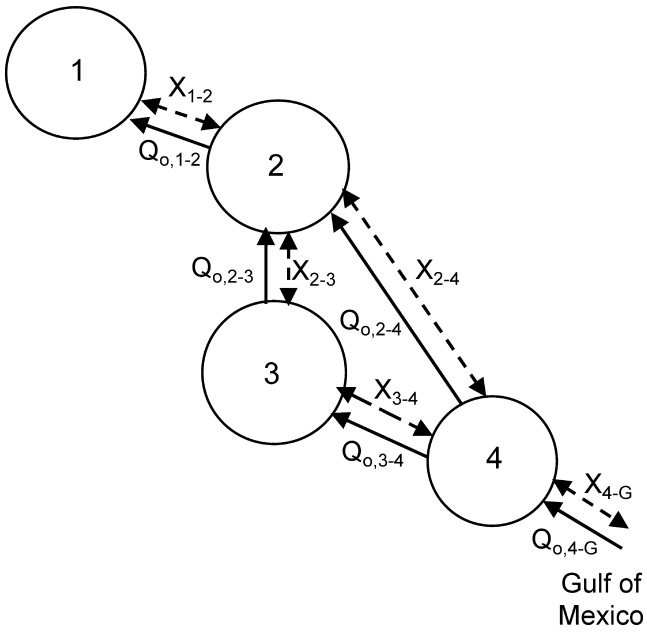

Figure 2. Schematic representation of a four-box mass balance model for the Barataria basin. Solid and dashed arrows represent advection and mixing flow exchanges, respectively.

rainfall is now the major source of fresh water to the Barataria basin. Annual average rainfall in the basin area is 160 cm, approximately, with significant intra-annual rainfall variability. On an annual basis, rainfall is in excess over evaporation. In addition to rainfall, fresh water into the basin has three other main sources: surface runoff from surrounding drainage basins, diversions from the Mississippi River (Naomi, West Point à la Hache, and Davis Pond), and the Gulf Intracoastal Waterway.

Salinity patterns and variations in the Barataria basin has been the subject of several data analyses and modeling studies (*e.g.,* GAGLIANO, MEYER-ARENDT, and WICKER, 1981; PARK, INOUE, and WISEMAN, 2002; SWENSON and TURNER, 1998; WISEMAN, SWENSON, and POWER, 1990). During times of high river flow, the effect of rainfall becomes unimportant, and salinities in the lower part of the basin are reduced because of the influence of the river plume on the salinity of coastal waters (ORLANDO *et al.,* 1993; WISEMAN and SWENSON, 1989). During times of low river flow, salinities increase and the effect of rainfall becomes more significant. For example, MCKEE, MENDELSSOHN, and MATERNES (2004) implicate a severe drought in 1998–2000 as a primary cause of high salinity values that contributed to an extensive die-off of wetland vegetation in the basin in 2000.

Salinity Calculations in a Mass Balance Model

We use a mass balance model to represent the assumed true relationship between rainfall and salinity in the Barataria basin. Mass balance models offer the advantage of computational efficiency and ease of implementation while providing a physically based description of the relationship between the net supply of fresh water and salinity (BABSON, KAWASE, and MCCREADY, 2006; HAGY, SANFORD, and BOYNTON, 2000; OFFICER, 1980). The model represents waterbodies in the Barataria basin as well-mixed subbasins linked by exchange flows that transport water and salt (Figure 2). The spatial and temporal averaging inherent in this representation prevents the mass balance model from capturing salinity variations that occur at tidal and synoptic (~0.1 per day) frequencies. However, applications across a number of systems including San Francisco Bay and Chesapeake Bay (*e.g.,* GIBSON and NAJJAR, 2000; UNCLES and PETERSON, 1996) suggest that such aggregated models can capture much of the salinity variation that occurs seasonally and from year to year. This is sufficient to forecast the effects of an altered salinity regime on the distribution of wetland communities within the Barataria basin with the ecological models that are presently available (VISSER *et al.,* 2003).

The mass balance model calculates the average salinity by keeping track of the changing amounts of water and salt in each subbasin (Figure 2; see Appendix for a detailed description of calculations performed by the model.) Monthly averages for rainfall, evapotranspiration, and the volumes of fresh water diverted from the Mississippi River drive the calculations. Monthly data on mean sea level and salinity describe boundary conditions at the mouth of Barataria Bay. The assembled input and boundary data cover the 11-year period of 1994 through 2004 (Figure 3). In addition to these input data, five parameters enter into the calculation of exchange fluxes among the subbasins and between the Barataria basin and coastal waters (Figure 2). One additional parameter, an evaporation coefficient similar to a pan coefficient, is used to calculate actual evapotranspiration rates over land areas as a fraction of the rate of potential evaporation.

Reference State

The reference state represents assumed true state of the system and is defined by the assumed true values for rainfall, salinity, and the model parameters that represent the relationship between rainfall and salinity. True values of mean areal rainfall for the basin are calculated by applying the Thiessen polygon point-to-area interpolation method (SINGH and CHOWDHURY, 1986) to rain gauge data from 12 sites (Figure 1). True values for the parameters in the salinity model (Table 1) are selected so that subbasin salinity values, calculated on the basis of the true mean area rainfall, reproduce the overall magnitude and patterns of variation in measured salinity values (Figure 3 and Table 2). The influence of tides and spatial variation within each subbasin, which are not accounted for by the model calculations, are evident in the comparison between calculated and observed values. The salinity values calculated from the reference state rainfall data and model parameters comprise the "true" values of salinity in each of the subbasins.

Sources of Uncertainty

Using the salinity model as a test bed for experimentation, we selectively contaminated with uncertainty the subbasin

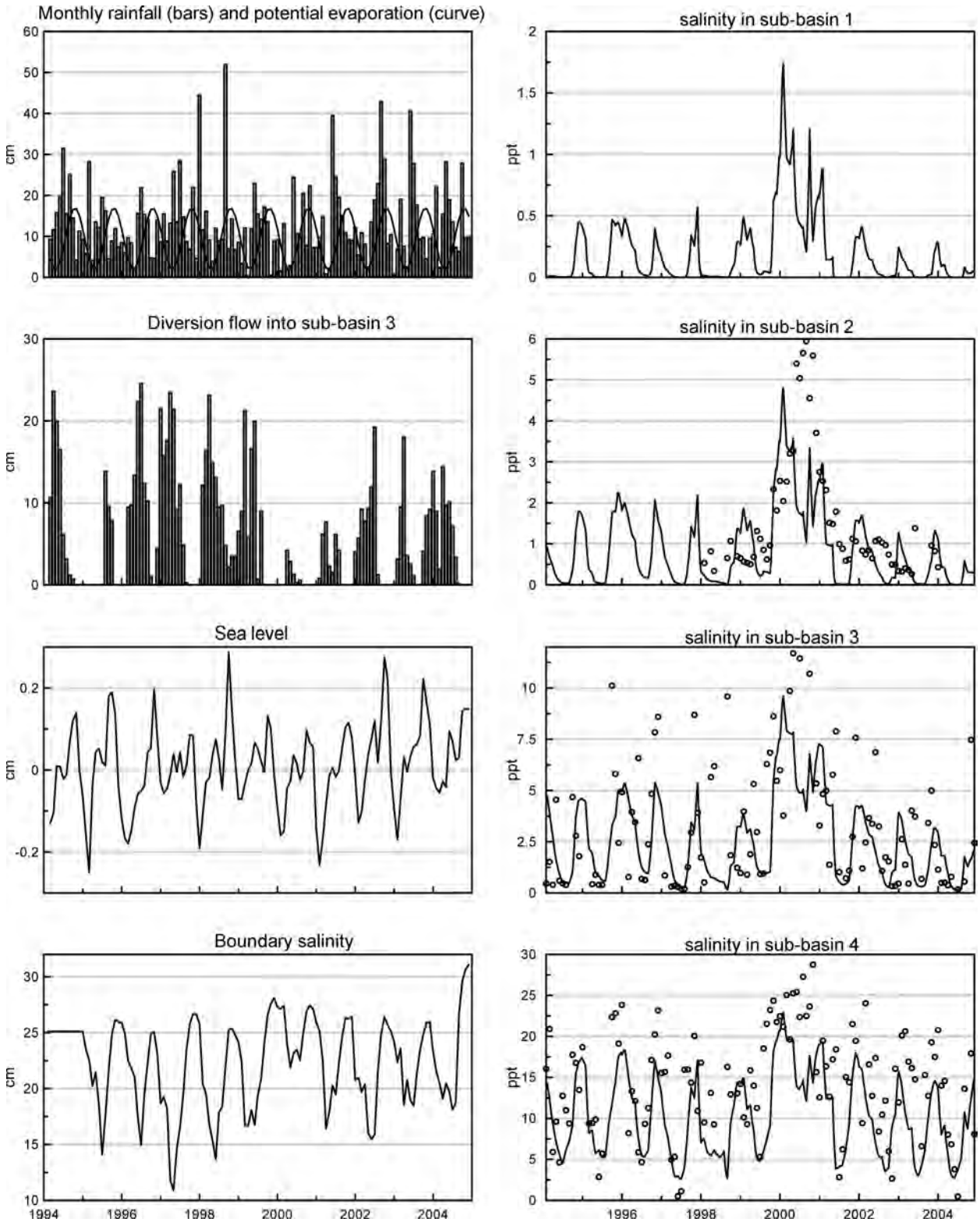

Figure 3. (Right panel) Salinity model predictions (continuous line) in the four subbasins corresponding to the "true" parameters of the reference run compared with actual salinity observations (circles). (Left panel) Examples of time series of hydrologic forcings for subbasin 3 (rainfall, potential evaporation, diversion flow) and other variables used to drive the reference run (gulf boundary salinity, and seawater level).

Table 1. *True parameters usd in the reference run and the feasible ranges assumed for the prior parameter distributions.*

	X_{1-2}	X_{2-4}	X_{3-4}	X_{2-3}	X_{4-G}	E_c
Reference true value	1.0	0.1	4.0	0.5	50	0.75
Prior range	0–300	0–300	0–300	0–300	0–300	0–1

Table 2. *Comparison of observed salinities and the corresponding values calculated by the calibrated box model used in this study to define the true reference state. Differences between observations and model calculations are quantified by the average of absolute differences. Actual salinity observations were not available in subbasin 1.*

	Average Salinity (ppt)		
Subbasin	Observed	Calculated	Absolute Difference
2	1.9	2.1	1.4
3	4.3	4.5	2.6
4	14.9	12.4	4.4

mean salinity and rainfall defined by the reference state. We then analyzed the effect that this introduced uncertainty had on the model parameters and the calculated salinity values. We next describe how such sources of uncertainty are simulated and introduced.

Simulation of Uncertainty in Salinity Data

Instrument errors are the most direct source of uncertainty in the salinity data used to calibrate the model. However, whereas the model provides subbasin average salinity predictions, the calibration data represent salinity at a much smaller scale, *i.e.,* as single-point measurements, providing another important source of uncertainty. Typically, uncertainty arising from instrumental errors will be small in the case of salinity measurements. However, uncertainty because of the mismatch between the model and observation scales, along with the effect of basin subscale salinity spatial variability, can be significant, especially in cases of sparse spatial sampling. In the case of Barataria basin, no more than one salinity measuring station was available in any of the four subbasins over the modeled period (11 y). However, salinity measurements at three stations in subbasin 2 were available for a limited number of years. These observations were analyzed to assess empirically the significance of spatial variability in salinity measurements. The standard deviation of differences between point and subbasin average salinities was found to be as high as 1 to 1.5 ppt. To study the effect of such uncertainty, we introduce normally distributed random errors with varying levels of variance into the subbasin salinity calibration data.

Another source of uncertainty in the salinity data arises from incomplete spatial coverage by the data available for model calibration. For example, in Barataria basin, continuous salinity observations were not available in subbasin 1 during the modeling period (1994–2005). This situation is typically encountered in many modeling applications, especially when extensive observational periods are needed. To address this issue, the reference salinity data used for model calibration are removed in one or more of the subbasins. Then, we assess the effect of such partially missing data on both the estimation of model parameters and the subsequent model predictions.

Simulation of Uncertainty in Rainfall Data

Among different freshwater sources, rainfall is one of the most challenging to quantify. This is attributed to two main reasons: insufficient spatial sampling and lack of accurate information on the magnitude of rainfall spatial variability. In the case of the Barataria basin, and in many other estuarine systems, rainfall sampling is sparse (approximately one gauge for every 500 km^2) (Figure 1). This introduces uncertainty in evaluating the mean areal rainfall required as input for salinity forecast calculations. Such uncertainty is enhanced where rainfall exhibits high natural spatial variability over scales comparable to the spacing between gauges.

The problem of characterizing uncertainty associated with estimation of mean areal rainfall with sparse sampling has been the subject of several studies in the last few decades. Geospatial methods and other approaches based on modeling spatial variability of rainfall have been developed and applied in earlier studies (*e.g.,* Bras and Rodriguez-Iturbe, 1985; Krajewski, 1987; Rodriguez-Iturbe and Mejia, 1974). In this study, an empirical approach is used to model the errors caused by the use of sparse rain gauge stations to estimate areal average rainfall. For illustration purposes, one scenario of rainfall sampling is examined herein in which areal average rainfall over each subbasin is estimated with a single rain gauge randomly located in the subbasin domain. A multiplicative model similar to that proposed by Krajewski (1987) and applied by Bradley *et al.* (2002) is used to describe the mismatch between observations of a single rain gauge located within the subbasin, R_g and the true areal rainfall averaged over the subbasin area, R_a,

$$R_g = \varepsilon(R_a)R_a \quad (1)$$

where $\varepsilon(R_a)$ is a random variable representing the error associated with estimating subbasin areal average rainfall with a single gauge. In this model, the error term, ε, depends on the true areal rainfall (R_a) and is described by a probability distribution, which can be estimated by analyzing a sample of simultaneous point and areal rainfall (R_g, R_a). As illustrated later in the Results section, we sample this distribution to generate realizations of the rainfall sampling error $\varepsilon(R_a)$, which are used in Equation (1) to introduce statistically representative uncertainty into the reference true values of R_a.

Uncertainty Analysis Scheme

Different scenarios of uncertainty in the input data (rainfall) and the calibration data (salinity) are analyzed. First, we examine three scenarios in which different types of uncertainty are introduced separately. In the first scenario, we introduce a normally distributed random error (with different variance values) into the subbasin salinity values. The second scenario introduces incomplete coverage of salinity monitor-

ing by omitting salinity values in selected subbasins from the calibration data. The third scenario introduces error into the subbasin rainfall values on the basis of the model described in Equation (1). Next, we examine the effects of different combinations of these three uncertainty scenarios.

For each scenario, we use an optimization and uncertainty analysis method known as the Shuffled Complex Evolution Metropolis (SCEM-UA) algorithm (DUAN, SOROOSHIAN, and GUPTA, 1992; VRUGT *et al.,* 2003). We use this method to propagate uncertainties introduced into rainfall and salinity data and to assess their effect on estimating the model parameters and on the predicted salinity values. The SCEM-UA algorithm is based on Markov Chain Monte Carlo (MCMC) techniques for Bayesian inference (GILKS, RICHARDSON, and SPIEGELHALTER, 1995), which have been applied increasingly in analysis of hydroecological and environmental systems (ENGELAND, XU, and GOTTSCHALK, 2005; OMLIN and REICHERT, 1999; QIAN *et al.,* 2003). Unlike classical statistics, Bayesian statistics treat the model parameters as random variables characterized by their probability density functions (OMLIN and REICHERT, 1999). Prior information on parameter distributions are then combined with observed data on state variables to provide improved and updated estimates of the parameter distributions. These updated distributions are often termed posterior distributions. Several recent application studies have demonstrated the utility of the SCEM-UA algorithm as a useful tool for estimating both the most likely parameter set and its posterior probability distribution (*e.g.,* HEIMOVAARA *et al.,* 2004; RAAT *et al.,* 2004; VRUGT, DEKKER, and BOUTEN, 2003). A full description of the algorithm is available in VRUGT *et al.* (2003), and only a brief description is given herein.

The algorithm starts with an initial population of parameter sets randomly sampled from an assumed predefined feasible probability distribution. The SCEM-UA runs a MCMC process long enough so that it eventually evolves to the posterior distribution of the model parameters after being updated according to the observed data. To estimate the posterior distribution of each parameter set, the SCEM-UA algorithm assumes that the model error residuals are mutually independent and normally distributed. This assumption was supported by examining the distribution of the mass balance model residuals after calibration against a set of actual monthly salinity observations in the Barataria basin. As such, the likelihood of a certain parameter set θ_i to describe the observed data *y,* $L(\theta_i|y)$, is defined by Equation (2),

$$L(\theta_i|y) = \exp\left[-\frac{1}{2}\sum_{j=1}^{n}\left|\frac{y_j - \hat{y}_j(\theta)}{\sigma}\right|^2\right] \quad (2)$$

where y denotes the available n number of measurements, $\hat{y}$ denotes the corresponding model predictions for the parameter set θ, and σ represents the error standard deviation of the measurements (monthly salinity values in this study).

The prior distributions of the model parameters were assumed uniform with a range that covers the feasible space of each parameter (Table 1). For each exchange flux parameter *X,* the range was set between 0 and 300. With respect to the true values of the parameters, the choice of such wide range is appropriate given that in real applications, little prior information is available on the actual parameter values. For the E_c evapotranspiration coefficient, the prior uniform range was selected between 0 and 1, which represents a feasible range for this parameter.

The SCEM-UA uses a quantitative criterion to check the convergence to a posterior distribution. In this study, the mass balance model is run for a total of 10,000 simulations for each uncertainty scenario. It was noted that in most cases, a stable posterior distribution was achieved after 5000 to 7000 model evaluations. After convergence, the most likely set of model parameters is identified. In addition, the calibrated sets of parameters in the last 3000 model simulations are considered to approximate the posterior distribution of the model parameters and can be used to describe the parameter uncertainty (*e.g.,* in terms of the 95% confidence interval).

These sets of parameters are subsequently used to generate different realizations of the model salinity output and to quantify the model prediction uncertainty. In addition to visual inspection of the time series of the last 3000 model simulations, their uncertainty was quantified with the statistical measures average bias, *B,* and average 95% uncertainty range, UR,

$$B = \frac{\frac{1}{n}\sum_{i=1}^{i=n}\left(\frac{1}{N}\sum_{j=1}^{j=N} M_{i,j} - O_i\right)}{\bar{O}} \quad (3)$$

$$\mathrm{UR} = \frac{\frac{1}{n}\sum_{i=1}^{i=n}(P_{97.5,i} - P_{2.5,i})}{\bar{M}} \quad (4)$$

where O_i is the "true" salinity observation at month i, $M_{i,j}$ is the corresponding model prediction for simulation j and month i, N is the number of model evaluations considered for deriving the posterior distribution ($N = 3000$), n is the number of months in the simulation period, $\bar{O}$ is the average observed salinity during n months, $P_{2.5,i}$ and $P_{97.5,i}$ are the 2.5 and 97.5 percentiles of the model results, respectively, computed from the N model simulations at each month i, and $\bar{M}$ is the average salinity model prediction computed by averaging $M_{i,j}$ over all $i = 1$ to n and $j = 1$ to N.

RESULTS

Effect of Uncertainty in Salinity Data

The likelihood function of Equation (2) makes it possible to incorporate information about uncertainty associated with the salinity calibration data through the error term σ. The size of this error reflects the reliability of the calibration data and how closely it represents the value of the variable. As such, large levels of σ will result in wider ranges of parameter sets that can provide acceptable fitting to the calibration data. This will subsequently cause wider uncertainty bounds in the model simulations.

Uncertainty in salinity data can be caused not only by random instrumental errors but, more importantly, by errors as a result of estimating subbasin mean salinity from point mea-

surements. As discussed earlier, analysis of salinity observations in one of the Barataria subbasins indicated that the standard deviation of these errors are in the range of 1 to 1.5 ppt. To assess effects of such uncertainty, different values of σ are considered: 0.1, 1, and 2 ppt. Although the case of σ = 0.1 ppt represents relatively low levels of uncertainty in the salinity data, the case of σ = 1 ppt represents more realistic errors that are associated with the use of point salinity data to calibrate the model. In addition, the case of σ = 2 is considered to investigate the effect of relatively large errors that might characterize the salinity measurements in other similar modeling situations. Examples of the results are given in Figure 4 for the case of σ = 2 ppt. The posterior distribution of each parameter is summarized in terms of its 95% uncertainty range for all σ cases, Table 3. The corresponding effect on the model simulations is also presented in terms of average bias (B) and average 95% uncertainty range (UR) calculated over the entire simulation period according to Equations (4) and (5).

As expected, small random errors in the calibration data (σ = 0.1 ppt) resulted in narrow uncertainty ranges in the retrieved parameters. The mean value of each parameter distribution was almost identical to the corresponding true parameter value, which resulted in negligible bias levels in the model simulations. The relatively narrow uncertainty bounds of the parameters also resulted in similarly narrow model uncertainty ranges. When σ was increased to 1 ppt, the parameter uncertainty ranges started to become wider, which has also caused rather considerable uncertainty in the model predictions, especially in subbasins 1 (44.5%) and 2 (17.5%). In this simulation the true values of X_{2-4} and X_{2-3} are not bounded within the 95% range, resulting in moderate levels of bias in the model predictions, especially in subbasin 1. Examining the case of σ = 2 ppt, which represents rather high errors in the calibration data, shows that the effect of calibration data errors on both the parameter retrieval and the accuracy of model predictions continued to increase. Model parameters had wide distributions, which caused significant model uncertainty ranges, especially in subbasins 1 (86.3%) and 2 (33.6%). Moreover, significant bias was observed with model predictions in subbasin 1 (18.7%). For all σ cases, both the bias and the uncertainty bounds of model predictions were much less significant for subbasins that are closer to the gulf boundary (subbasins 3 and 4) than in the inland subbasins (1 and 2). The effect was also most evident for subbasin 1 because of its relatively low salinity values compared with the introduced random errors.

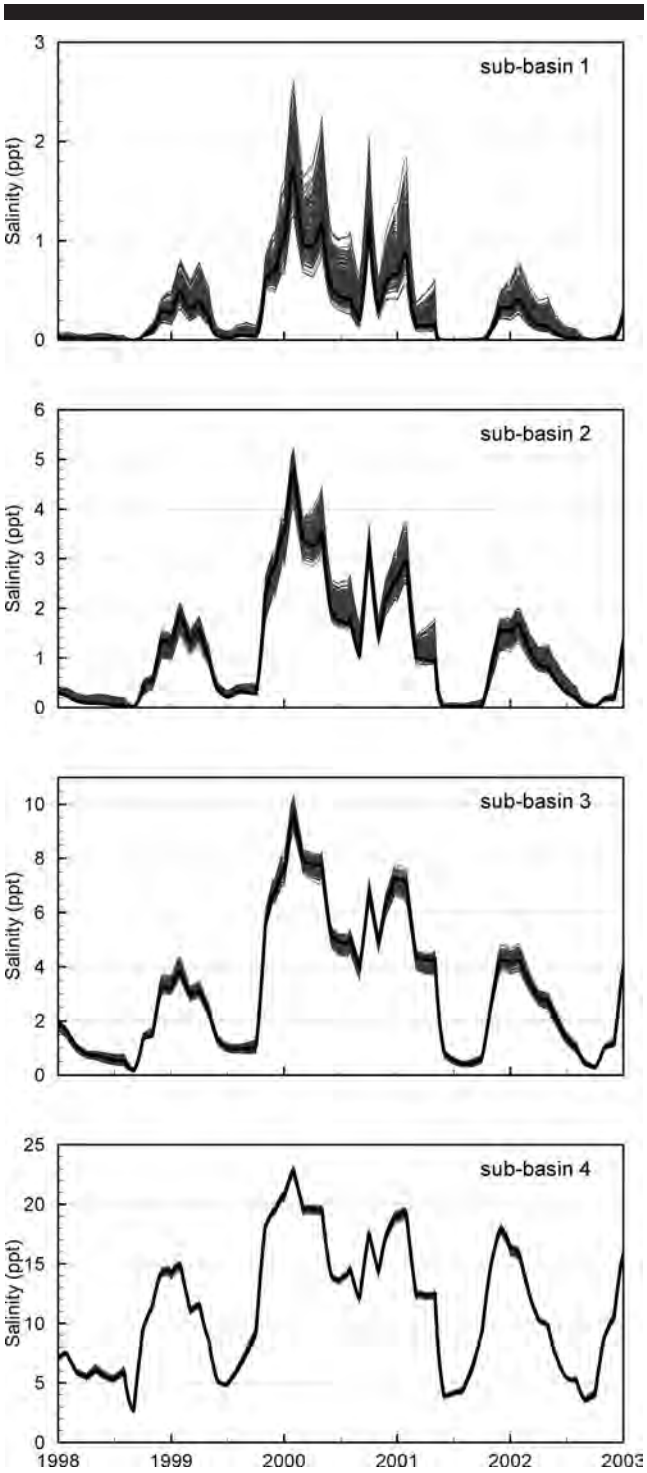

Figure 4. Model salinity predictions associated with the case of introducing random errors in the salinity calibration data (σ = 2 ppt). Results are shown from the last 3000 simulations after convergence of the SCEM-UA algorithm. The dark line represents the reference run with "true" model parameters.

Effect of Incomplete Coverage in Salinity Data

Next we analyze the effect of incomplete coverage of salinity monitoring in some of the subbasins. For illustration purposes, this analysis was performed for two scenarios of partially incomplete calibration data. The first scenario is the case of missing data in one subbasin (subbasin 1 in the Barataria basin) and represents an example of common problems of missing data. The second scenario assumes missing data in two subbasins (1 and 4). This scenario represents an extreme case of incomplete calibration data that might be en-

Table 3. *The 95% confidence intervals of model parameters and average bias (*B*) and 95% uncertainty ranges (UR) of model predictions as the result of different levels of calibration random errors.* B *and UR statistics are shown for the four subbasins 1, 2, 3, and 4. Statistics are computed from the last 3000 model simulations. Values in Parentheses are true reference parameter values.*

SD of Error (ppt)	Model Parameter 95% Confidence Interval						Model Prediction							
							Average Bias B (%)				Average 95% UR (%)			
	X_{1-2} (1.0)	X_{2-4} (0.1)	X_{3-4} (4)	X_{2-3} (0.5)	X_{4-G} (50)	E_c (0.75)	1	2	3	4	1	2	3	4
0.1	0.73–1.24	0.06–0.14	3.9–4.1	0.33–0.73	49.7–50.3	0.748–0.752	−0.1	0	0	0	5.8	2.1	0.7	0.2
1.0	0.14–4.3	0.13–0.48	2.8–5.8	0.71–4.53	47.7–52.6	0.73–0.77	7.3	1.5	0	0	44.5	17.5	6.7	2.0
2.0	0.26–8.6	0.13–0.79	2.6–7.8	1.3–10.7	46.8–56.6	0.70–0.77	18.7	4	0	0.1	86.3	33.6	13.3	4.1

countered in poorly monitored systems. The two scenarios were tested under different levels of salinity calibration data errors (0.1, 1, and 2 ppt) to examine the interaction of these two different sources of uncertainty. Examples of the results are given in Figure 5 for the case of missing data in subbasin 1, with $\sigma = 1$ ppt. A statistical evaluation of the three analyzed error levels is presented in Table 4. In general, missing calibration data in subbasin 1 had the most significant effect on the estimation of parameter X_{1-2} and on the model predictions in subbasin 1. This effect was significantly augmented when the value of calibration random errors increased from 0.1 to 1 and 2 ppt. As such, parameter X_{1-2} could not be estimated with any precision (the estimated confidence interval was nearly as wide as the prior assumed range of 0 to 300). Moreover, the average bias and 95% uncertainty range of model predictions attained significantly large values of 132% and 342%, respectively, in the case of $\sigma = 1.0$ ppt, and 284% and 88.6%, respectively, in the case of $\sigma = 2.0$ ppt.

The second scenario, in which calibration data were not available in both subbasins 1 and 4 (Table 5), was investigated with three values of σ. This scenario was compared against two other scenarios: uncertainty because of missing data in subbasin 1 only and uncertainty because of calibration random errors only. In contrast to other uncertainty scenarios examined before, this scenario has affected the retrieval of most of the model parameters, especially with $\sigma = 1$ or 2 ppt. The parameter posterior distributions have become significantly wider for parameters X_{4-G}, which controls flow exchanges between the gulf and the adjacent subbasin, and E_c, which determines the volume of fresh water lost through evapotranspiration. The effect on model predictions in terms of both the bias and the uncertainty bounds was also amplified because of the additional lack of data in subbasin 4. It is interesting to notice that, although most model parameters were affected by lack of calibration data in subbasin 4, model predictions in subbasins 3 and 4 were less affected than the two most inland subbasins (1 and 2). This pattern can be explained by the possibility that parameters X_{4-G} and E_c compensated for each other in such a way to respect the imposed salinity at the Gulf southern boundary condition of the model. In support of this interpretation, the posterior distributions of the parameters X_{4-G} and E_c showed a relatively high correlation coefficient.

Effect of Insufficient Rainfall Sampling

Rainfall exhibits a high degree of spatial variability on the scale of the Barataria basin. This combined with the relatively sparse coverage by rain gauges introduces uncertainty into estimates of basin average rainfall required for salinity predictions. As described earlier, this uncertainty can be represented through the error term (ε) that measures differences between subbasin mean rainfall (R_a) and measurements of a single rain gauge station (R_g) [Equation (1)]. The probability distribution of the error term is estimated by analyzing the (R_g, R_a) joint sample assembled from rainfall data for the 11-year period 1994 through 2004. A sample of R_g is readily obtained from rain gauge data within each subbasin. The subbasin reference state rainfall R_a is derived by applying the Thiessen polygons interpolation method with data from all available rain gauges in each subbasin. The error term (ε), computed as the ratio R_g/R_a, exhibits a clear dependence on the magnitude of R_a, (Figure 6a), decreasing sharply as R_a increases. Analysis of the empirical probability distribution of ε indicated that it could be reasonably modeled with a log-normal distribution described by its first two moments, the mean $E\{\varepsilon\}$, or μ_ε, and the variance $\mathrm{Var}\{\varepsilon\}$, or σ_ε^2. However, to account for the dependency of ε on R_a, these two moments should be conditionally characterized: $\mu_{\varepsilon|R_a}$ and $\sigma^2_{\varepsilon|R_a}$. A similar approach was recently applied by CIACH and GIEBREMICHAEL (2004) to model uncertainty in radar rainfall estimates. The (R_a, R_g) sample was partitioned into subsamples

Table 4. *Same as in Table 3 but for the case of missing calibration data in subbasin 1 under different levels of calibration random errors. Values in parentheses are true reference parameter values.*

SD of Error (ppt)	Model Parameter 95% Confidence Interval						Model Prediction							
							Average Bias B (%)				Average 95% UR (%)			
	X_{1-2} (1.0)	X_{2-4} (0.1)	X_{3-4} (4)	X_{2-3} (0.5)	X_{4-G} (50)	E_c (0.75)	1	2	3	4	1	2	3	4
0.1	0.22–2.4	0.07–0.14	3.9–4.1	0.35–0.71	49.7–50.3	0.74–0.75	2.4	0.1	0	0	26.6	2.4	0.73	0.2
1.0	0.46–254.9	0.08–0.56	2.5–5.7	0.32–3.86	47.5–53	0.72–0.77	132	2.6	−1	0	342	19	7.5	2
2.0	9.04–267.7	0.20–1.04	2.0–7.1	1.4–10.5	46.1–55.4	0.71–0.79	284	7	0.5	0	88.6	37.6	13.2	4.1

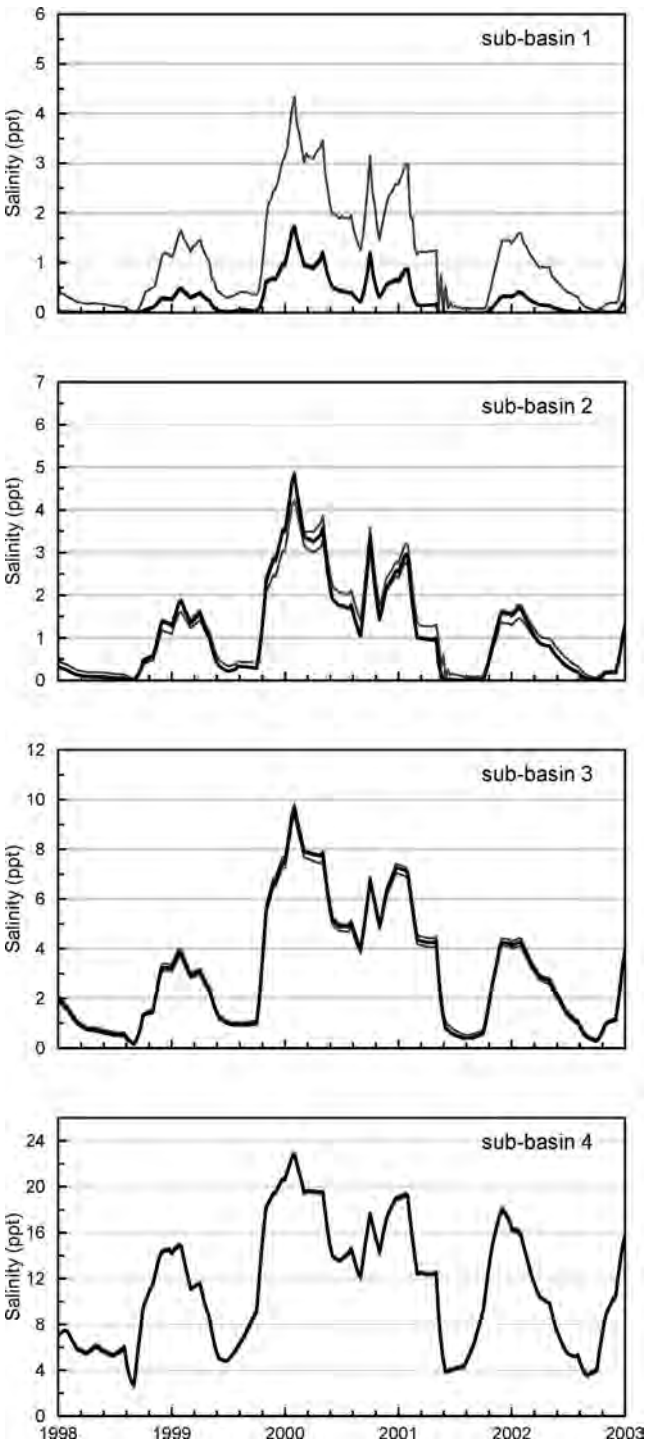

Figure 5. The 95% uncertainty ranges of model salinity predictions as a result of missing calibration data in subbasin 1 and calibration random errors with $\sigma = 1$ ppt. The dark line represents the reference run with "true" model parameters (for this particular uncertainty case, the lower uncertainty range of salinity predictions in subbasin 1 coincides with the reference run).

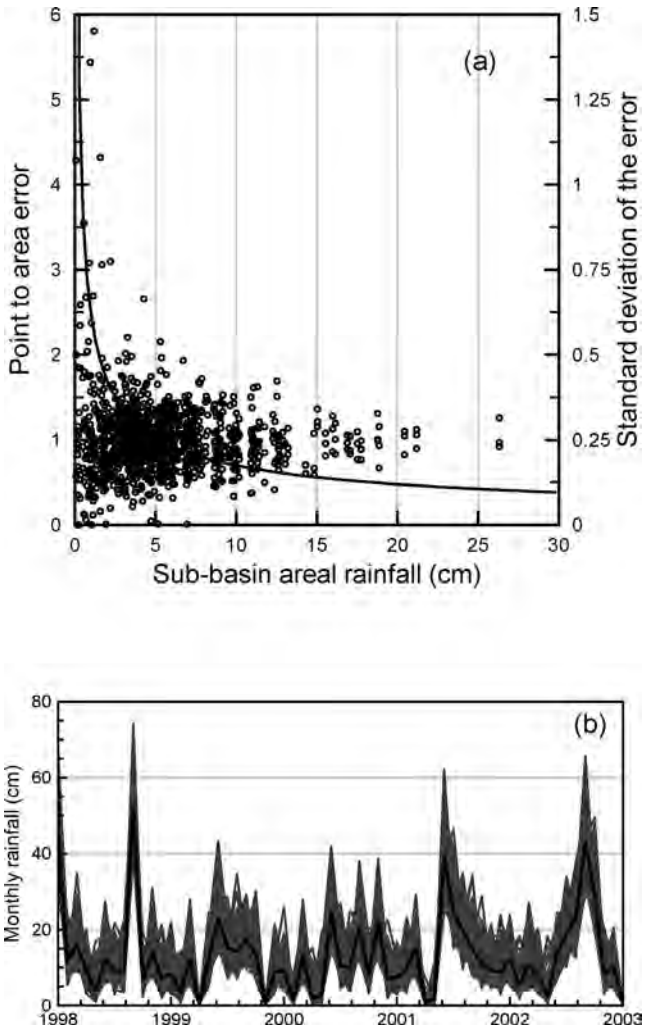

Figure 6. (a) Scatter plot of the areal rainfall estimation error ε *vs.* the corresponding areal rainfall R_a. The solid line indicates the fitted function of the conditional standard deviation of ε. (b) An example of 500 realizations of rainfall time series generated for subbasin 3 by the rainfall empirical model. The dark line represents "true" rainfall used to generate the realizations.

conditioned on R_a, and the means and the standard deviations of these subsamples were computed. As expected $\mu_{\varepsilon|R_a}$ was close to 1 for all ranges of R_a but $\sigma^2_{\varepsilon|R_a}$ decreased with the increase of R_a as shown in Figure 6a. The dependence of $\sigma^2_{\varepsilon|R_a}$ can be conveniently approximated as shown in Figure 6a by Equation (5),

$$\sigma^2_{\varepsilon|R_a} = \alpha(R_a)^{-\beta} \quad (5)$$

where α and β are empirical fitting coefficients. An example of 500 realizations of rainfall time series generated for subbasin 3 is shown in Figure 6b. The generated realizations are unbiased as a result of the imposed condition $\mu_{\varepsilon|R_a} = 1$.

Thousands of statistically possible time series realizations of point rainfall observations for each subbasin in the Barataria estuary were generated by sampling from the lognormal

Table 5. *Same as in Table 4 but for the case of missing calibration data in subbasins 1 and 4. Values in parentheses are true reference parameter values.*

SD of Error (ppt)	Model Parameter 95% Confidence Interval						Model Prediction							
							Average Bias B (%)				Average 95% UR (%)			
	X_{1-2} (1.0)	X_{2-4} (0.1)	X_{3-4} (4)	X_{2-3} (0.5)	X_{4-G} (50)	E_c (0.75)	1	2	3	4	1	2	3	4
0.1	0.05–1.74	0.05–0.27	3.8–13.4	0.28–1.67	13.6–49.8	0.75–0.82	−5.4	−3.8	−1	−15	39.8	15.7	10.2	28.6
1.0	1.25–259.5	0.10–0.54	1.4–7.8	0.46–4.5	36.3–68.3	0.70–0.78	138	2.6	0.5	−0.2	200	22.4	10.2	20.2
2.0	2.7–291	0.13–1.38	0.9–16.7	2.2–15.4	26.8–71	0.65–0.79	267	8	1	3	204	40.3	20.2	28.6

distribution described previously. Each time series realization was then used as input to the mass balance model. The SCEM-UA algorithm was applied to estimate the posterior probability distributions of the model parameters. Distributions of each parameter were then merged from all realizations to provide a distribution that reflects the effect of uncertain rainfall input. These parameter sets were used to run the model and analyze the salinity predictions in each subbasin.

The most obvious effect of rainfall uncertainty is in the increased uncertainty ranges of all parameters. The analysis was performed for the three error levels of the salinity calibration data as considered earlier: $\sigma = 0.1$, 1, and 2 ppt. An example of the results obtained with $\sigma = 0.1$ ppt is shown in Figure 7. A statistical summary of the three σ cases is given in Table 6. Unlike scenarios in which uncertainty was introduced only through random errors in calibration data (Table 3), the uncertainty ranges of all parameters (including E_c) have become significantly wide. Because E_c controls how much fresh water is lost from each subbasin through evapotranspiration, the increase in its uncertainty range can be explained by the attempt of the calibration procedure to compensate for deviations of the uncertain rainfall input from the "true" rainfall information. Such compensation was evident in the relatively high correlations between the probability distribution of E_c and those of two of the other model parameters (X_{3-4} and X_{4-G}).

The wide parameter uncertainty ranges resulted in a significant increase in the uncertainty of model predictions. Predictions in the four subbasins attained relatively wide uncertainty bounds regardless of the assumed error level in the salinity calibration data. The introduction of rainfall estimation uncertainty alone or with negligible calibration data random errors did not cause any significant biases in the model simulations (<1.8% for all subbasins) because the error model used to simulate rainfall estimation uncertainty preserves total rainfall volume (rainfall estimates with Equation (1) are unbiased with $\mu_{\varepsilon|R_a} = 1$). Only when the error levels of the calibration data increased ($\sigma = 1$ or 2 ppt) do biases in the simulated salinities start to be significant.

Effect of Combined Sources of Uncertainty

It is not generally understood how different sources of variation and error interact to determine the total uncertainty in model predictions (ENGELUND, XU, and GOTTSCHALK, 2005). To investigate this interaction, the separate sources of uncertainty analyzed before are introduced simultaneously, and their combined effect on parameter estimates and salinity predictions is compared with the results of each error acting separately. The analysis examines the combined effect of uncertainty in the salinity calibration data ($\sigma = 1$ ppt), salinity data missing in subbasin 1, and the uncertainty of estimating rainfall from a single gauge in each subbasin (Figure 8 and Table 7).

The comparison suggests that different sources of uncertainty combine in such a way as to amplify their separate effects, at least in one part of the model domain. The uncertainty range for the parameter X_{1-2} is now much wider (0.68 to 290) than in any of the individual uncertainty cases. The 95% uncertainty ranges for predicted salinity in subbasin 1 increases dramatically to 569% under the combined scenario compared with 4.4%, 2.9%, and 186% when the effects of uncertainty in the calibration data, missing data, and uncertainty in rainfall, respectively, were introduced separately. Similarly, the level of bias increases significantly from 7.3%, −0.04%, and 1.39% for the separate sources to 255% when they are combined. The effects of the combined scenario are not as pronounced for predictions in the other subbasins where the total uncertainty appears to be determined mostly by the uncertainty in rainfall estimates.

DISCUSSION

In this study, we demonstrated the kind of information that uncertainty analysis can provide to managers charged with the protection and restoration of estuarine systems. Of the three sources of uncertainty investigated here, the uncertainty in area average rainfall volumes has the most significant effect on salinity predictions in the Barataria basin. The use of sparse rain gauge stations to estimate average rainfall over the subbasin area lead to unidentifiable model parameters, which has in turn caused large uncertainty in the model predictions. In the upper portion of the basin, subbasin 1, salinity predictions are also sensitive to the effect of incomplete coverage by the available salinity data. Therefore, efforts to improve predictions should investigate the advantages of alternative approaches to compiling the rainfall estimates needed to predict salinity, and salinity monitoring should be expanded into the upper portion of the basin if accurate predictions are required here. A more complete analysis of uncertainty likely will uncover other factors that should also be considered. The results of this study pointing to the importance of rainfall imply that uncertainty in evaporation estimates, which were not considered in this study, might be another important source of uncertainty in salinity predictions. Rainfall and evaporation are major components in the freshwater budget of the basin, and they are similar

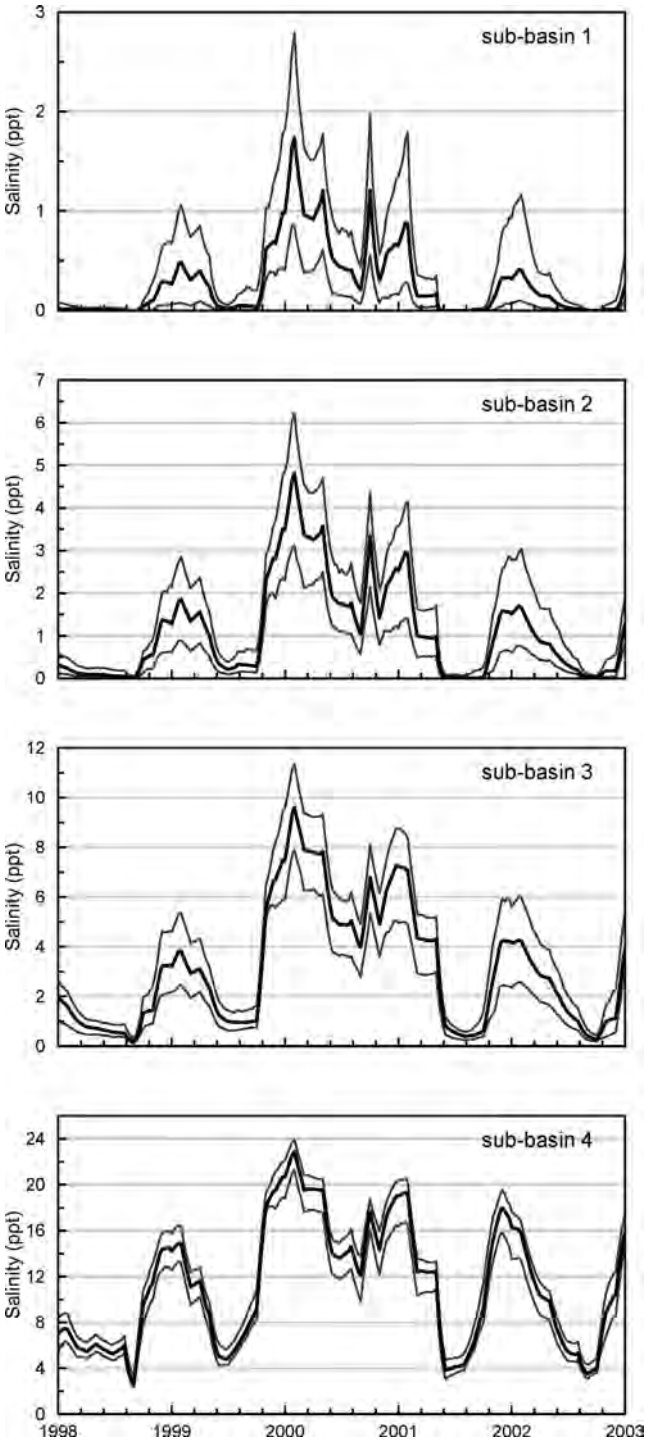

Figure 7. The 95% uncertainty ranges of model salinity predictions associated with the case of uncertain rainfall input and $\sigma = 0.1$ ppt. Different input rainfall realizations, generated with the rainfall model error, were used to simulate rainfall estimation uncertainty. The dark line represents the reference run with "true" area average rainfall.

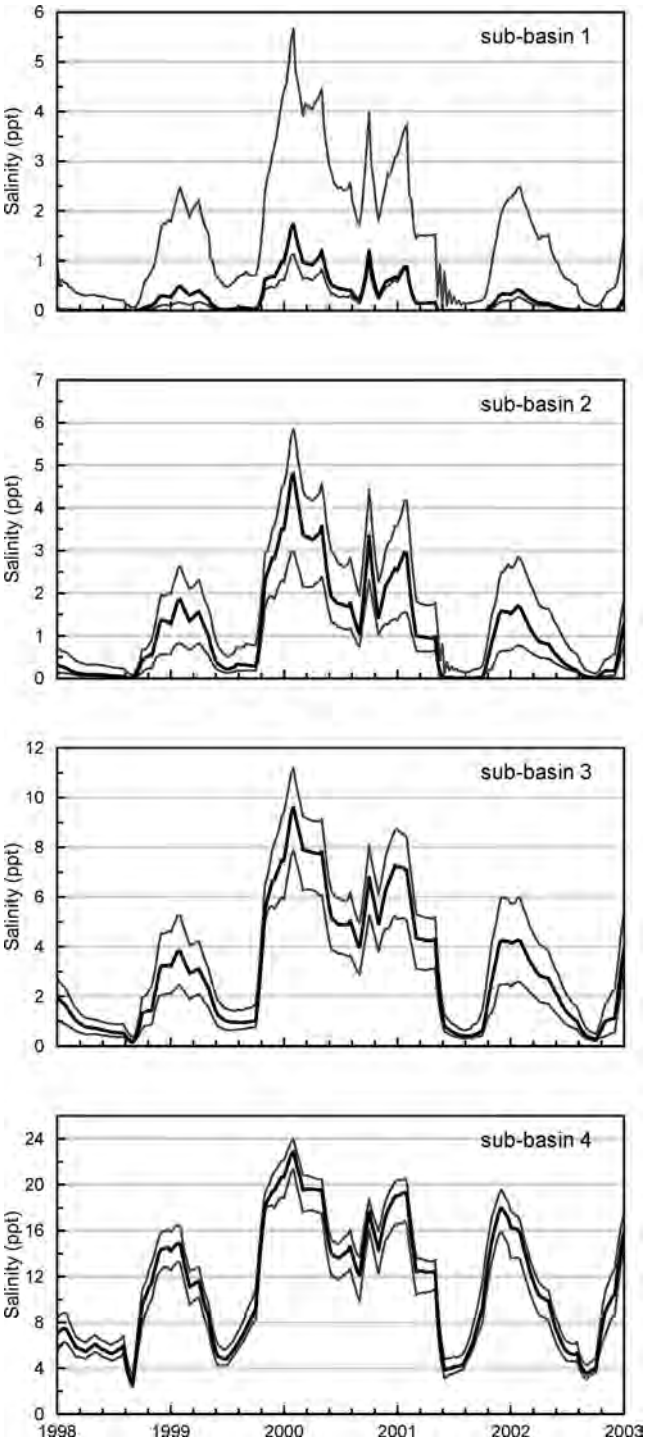

Figure 8. Uncertainty ranges of model salinity predictions associated with combined sources of uncertainty: imperfect rainfall input, random errors in calibration data ($\sigma = 1$ ppt), and calibration data unavailable in subbasin 1. The dark line represents the reference run with "true" area average rainfall.

Table 6. *Effect of errors in estimating areal average rainfall on uncertainties of model parameters and simulations. Values in parentheses are true reference parameter values.*

SD of Error (ppt)	Model Parameter 95% Confidence Interval						Model Prediction							
							Average Bias B (%)				Average 95% UR (%)			
	X_{1-2} (1.0)	X_{2-4} (0.1)	X_{3-4} (4)	X_{2-3} (0.5)	X_{4-G} (50)	E_c (0.75)	1	2	3	4	1	2	3	4
0.1	0.01–3.4	0.02–0.87	3.1–9.7	0.1–6.38	48.6–64	0.65–0.82	1.8	−0.4	−0.1	−0.1	186	104	64	23
1.0	0.1–5.18	0.13–0.92	2.9–10.3	0.86–8.86	48.9–64.8	0.65–0.82	8.9	0.7	−0.1	−0.1	195	103	64	23
2.0	0.18–10.5	0.09–1.07	2.7–11.7	1.46–14.0	48.5–66.8	0.65–0.82	23	2.5	−0.2	0	218	104	65	23

in magnitude and in their effect on estuarine salinity (SUMMER AND BELAINEH, 2005). A complete evaluation of uncertainty in salinity forecasts should include an analysis of the uncertainty in evapotranspiration and other factors not considered here, such as the influence of Mississippi River flow on salinity at the mouth of the basin (*e.g.,* WISEMAN and SWENSON, 1989).

The results of this study are valid only as long as the estuarine system in the Barataria basin does not differ drastically from its state during the period 1994 through 2004, as described by the available data and by the models used to interpret these data. The diversion of even a small proportion of the total discharge of the Mississippi River into the Barataria basin would alter the system beyond our ability to forecast its response, except in only the most general terms. The average flow from the diversions at Davis Pond, Naomi, and West Point à la Hache (Figure 1) in the period 1994 to 2004 amounts to only about 0.1% of the Mississippi River discharge. At only 1% of the river discharge, the diversion inflow would exceed the present input of fresh water from rainfall and increase the annual net supply of fresh water to the basin by a factor of four or five. To forecast how the estuarine ecosystem would respond to much higher diversion inflows can only be accomplished through comparative analysis (*e.g.,* FERREIRA *et al.,* 2005; SOLIS and POWELL, 1999). As a practical matter, such drastic restoration measures are still several years in the future. In the meantime, resource managers can increase the diversion of water and sediment from the Mississippi River into Barataria basin through existing structures without driving the estuarine system to change unpredictably. For example current operations limit inflow at Davis Pond (Figure 1) well below the design capacity of the structure. Even at the structure's full capacity (~10,000 ft^3/s [~300 m^3/s]) inflow through this diversion would not exceed the input of fresh water to the basin from rainfall. The subsidy to the net supply of fresh water in the basin by the increases in diversions that are achievable within the next several years are comparable to the magnitude of variation between wet years and dry years. It should be possible to forecast the response of the estuarine system to this level of change, but we must evaluate the uncertainty inherent in these forecasts and identify the critical information needed to reduce this uncertainty.

CONCLUSIONS

In this paper, we presented uncertainty analyses of salinity predictions provided by a mass balance box model for a coastal estuarine system. A Bayesian-based optimization and uncertainty analysis algorithm was used to study the effect of different sources of uncertainty on estimating model parameters and on the uncertainty of subsequent model predictions. The performed analyses focused on uncertainty as a result of random errors in calibration data, lack of sufficient coverage in calibration data, and uncertainty associated with estimating hydrologic forcing inputs. A simulation framework enabled us to assess the effects of individual as well combined sources of uncertainty. The results indicated that the examined error sources lead to significantly wide posterior distributions of the model parameters. In some cases, the posterior distribution was as wide as the prior assumed feasible range of the parameter. Lack of calibration data in certain areas of the model domain caused moderate to large biases and random errors in the model predictions. It is worth noting that although model parameters were characterized with relatively wide uncertainty ranges, they compensated for each other

Table 7. *Effect of combined sources of uncertainties compared with individual unceratinty cases. (i) Errors in calibration data with σ = 1 ppt, (ii) missing calibration data in subbasin 1, and (iii) uncertain rainfall input. Values in parentheses are true reference parameter values.*

Case	Model Parameter 95% Confidence Interval						Model Prediction							
							Average Bias B (%)				Average 95% UR (%)			
	X_{1-2} (1.0)	X_{2-4} (0.1)	X_{3-4} (4)	X_{2-3} (0.5)	X_{4-G} (50)	E_c (0.75)	1	2	3	4	1	2	3	4
(i)	0.14–4.3	0.13–0.48	2.8–5.8	0.71–4.53	47.7–52.6	0.73–0.77	7.3	1.5	0	0	44.5	17.5	6.7	2.0
(ii)	0.88–1.1	0.09–0.1	3.9–4.0	0.47–0.53	49.9–50.0	0.74–0.75	−0.04	0	0	0	2.9	0.24	0.08	0.02
(iii)	0.01–3.3	0.01–0.87	3.1–9.7	0.08–6.33	48.7–63.9	0.65–0.81	1.39	−0.5	−0.1	−0.1	186	104	64.6	23
(i) and (ii)	0.46–255	0.08–0.56	2.5–5.7	0.32–3.86	47.5–53	0.72–0.77	132	2.6	−1	0	342	19	7.5	2
(i) and (iii)	0.1–5.1	0.13–0.92	2.9–10.3	0.86–8.86	48.9–64.8	0.65–0.82	8.9	0.7	−0.1	−0.1	195	103	64	23
(ii) and (iii)	0.01–300	0.01–0.86	2.3–9.6	0.03–6.2	47.4–63.5	0.66–0.83	199.0	1.4	0.5	−0.1	598	105	63.8	23.7
(i), (ii), and (iii)	0.7–290	0.09–1.0	2.1–9.7	0.4–7.8	47.5–63.9	0.66–0.83	255	3.3	0.4	−0.1	569	104	63.8	23.7

such that model predictions still matched the reference salinity values in some of the subbasins.

Although this study was conducted for a particular estuarine system, the results obtained herein and the applied methodologies have broader implications for other systems. The use of a simulation framework, in which the response of the system is known exactly, as an analog for the real world can help resource managers design monitoring systems and identify data and information gaps in the variables of interest in coastal restoration programs. This strategy is particularly important in monitoring complex estuarine systems in which limited equipment and human resources are available.

ACKNOWLEDGMENT

This study was supported by the Louisiana Department of Natural Resources through the Coastal Louisiana Ecosystem Assessment and Restoration (CLEAR) program. We thank Eric Swenson and Dubravko Justic (Coastal Ecology Institute–Louisiana State University) for compiling and sharing the salinity data sets used to calibrate and validate the salinity box model. Analysis by the SCEM-UA method was performed on the basis of a modified version of a MATLAB program provided by Dr. Jasper A. Vrugt; his insightful discussions on the use of the SCEM-UA method are acknowledged. This paper is dedicated to the memory of Dr. E. Barry Moser (Head, Department of Experimental Statistics, Louisiana State University).

LITERATURE CITED

Babson, A.L.; Kawase, M., and McCready, P., 2006. Seasonal and interannual variability in the circulation of Puget Sound, Washington: a box model study. *Atmosphere-Ocean* 44(1), 29–45.

Boesch, D.F.; Josselyn, M.J.; Mehta, A.J.; Morris, J.T.; Nuttle, W.K.; Simenstad, C.A., and Swift, D.J.P., 1994. Scientific assessment of coastal wetland loss, restoration and management in Louisiana. *Journal of Coastal Research,* Special Issue No. 20, pp. 1–103.

Bradley, A.A.; Peters-Lidard, C.D.; Nelson, C.B.R.; Smith, J.A., and Young, C.B., 2002. Raingauge network design using NEXRAD precipitation estimates. *Journal of the American Water Resources Association,* 38(5), 1393–1407.

Bras, R.L. and Rodriguez-Iturbe, I., 1985. *Random Functions and Hydrology.* New York: Addison-Wesley, 559p.

Ciach, G. and Gebremichael, M., 2004. Empirical modeling of the uncertainties in radar rainfall estimates. *In: Proceedings of the 6th International Symposium on Hydrological Applications of Weather Radar* (Melbourne, Australia, Bureau of Meteorology and Australian Meteorological and Oceanographic Society), CD.

Coleman, J.M.; Robert, H.H., and Stone, G.W. 1998. Mississippi River delta: an overview. *Journal of Coastal Research,* 14, 698–716.

Delaune, R.D.; Jugsujinad, A.; West, J.L.; Johnson, C.B., and Kongchum, M., 2005. A screening of the capacity of Louisiana freshwater wetlands to process nitrate in diverted Mississippi River water. *Ecological Engineering,* 25(4), 315–321.

Duan, Q.Y.; Sorooshian, S., and Gupta, V., 1992. Effective and efficient global optimization for conceptual rainfall-runoff models. *Water Resources Research,* 28, 1015–1031.

Engelund, K.; Xu, C., and Gottschalk, L., 2005. Assessing uncertainties in a conceptual water balance model using Bayesian methodology. *Hydrological Sciences Journal,* 50(1), 45–63.

Ferreira, J.G.; Wolff, W.J.; Simas, T.C., and Bricker, S.B., 2005. Does biodiversity of estuarine phytoplankton depend on hydrology? *Ecological Modeling,* 187, 513–523.

Fitzgerald, D.M.; Kulo, M.; Penland, S.; Flocks, J., and Kindinger, J., 2004. Morphologic and stratigraphic evolution of muddy ebb-tidal deltas along a subsiding coast: Barataria Bay, Mississippi River delta. *Sedimentology,* 51: 1157–1178.

Gagliano, S.; Meyer-Arendt, K., and Wicker. K., 1981. Land loss in the Mississippi River deltaic plain. *Transactions of the Gulf Coast Association of Geological Societies,* 31, 295–300.

Gibson, J.R. and Najjar, R.G., 2000. The response of Chesapeake Bay salinity to climate-induced changes in streamflow. *Limnology and Oceanography,* 45, 1764–1772.

Gilks, W.R.; Richardson, S., and Spiegelhalter, D.J., 1995. Introducing Markov chain Monte Carlo. *In:* Gilks, W.R., Richardson, S., and Spiegelhalter, D.J. (eds), *Markov Chain Monte Carlo in Practice.* London: Chapman & Hall, pp. 1–19.

Hagy, J.D.; Sanford, L.P., and Boynton, W.R., 2000. Estimation of net physical transport and hydraulic residence times for a coastal plain estuary using box models. *Estuaries,* 23(3), 328–340.

Heimovaara, T.J.; Huisman, J.A.; Vrugt, J.A., and Bouten, W., 2004. Obtaining the spatial distribution of water content along a TDR probe using the SCEM-UA Bayesian inverse modeling scheme. *Vadose Zone Journal,* 3(4), 1128–1145.

Houck, O., 2006. Can we save New Orleans? *Tulane Environmental Law Journal* 19, 1–68.

Krajewski, W.F., 1987. Co-kriging of radar-rainfall and rain gauge data. *Journal of Geophysical Research–Atmospheres,* 92(D8), 9571–9580.

Lall, U.; Philips, D.L.; Reckhow, K.H., and Loucks, D.P., 2002. Quantifying and Communicating Uncertainty for Decision Making in the Everglades. Report of the Comprehensive Everglades Restoration Plan's Model Uncertainty Workshop. West Palm Beach, Florida: US Army Corps of Engineers, South Florida Water Management District.

Mckee, K.L.; Mendelssohn, I.A., and Materne, M.D., 2004. Acute salt marsh dieback in the Mississippi River deltaic plain: a drought-induced phenomenon? *Global Ecology and Biogeography,* 13, 65–73.

NRC (National Research Council), 2002. Risk Analysis and Uncertainty in Flood Damage Reduction Studies. Committee on Risk-Based Analysis for Flood Damage Reduction. Water Science and Technology Board, Commission on Geosciences, Environment, and Resources, NRC. Washington, DC: National Academy Press.

Officer, C.B., 1980. Box models revisited. *In*: Hamilton, P., and Macdonald, R.B. (eds.), *Estuarine and Wetland Processes. Marine Sciences Series,* Volume 11. New York: Pelnum Press, pp. 65–114.

Omlin, M. and Reichert, P., 1999. A comparison of techniques for the estimation of model prediction uncertainty. *Ecological Modelling* 115, 45–59.

Orlando, S.P.; Rozas, L.P.; Ward, G.H., and Klien, C.J., 1993. Salinity Characterization of Gulf of Mexico Estuaries. Silver Spring, MD: Office of Ocean Resources Conservation and Assessment, National Oceanic and Atmospheric Administration, 209p.

Park, D.; Inoue, M., and Wiseman, W.J., Jr., 2002. A high-resolution integrated hydrology-hydrodynamic model of the Barataria basin system. Proceedings of Conference of OCEANS 2002 MTS/IEEE Meeting (Biloxi, Mississippi, MTS/IEEE), October 2002, pp. 1234–1242.

Penland, S.; Boyd, R., and Sutter, J.R. 1988. Transgressive depositional systems of the Mississippi Delta plain: model for barrier shoreline and shelf sand development. *Journal of Sedimentary Research,* 58, 932–949.

Qian, S.; Craig, S.; Stow, A., and Borsuk, M.E., 2003. On Monte Carlo methods for Bayesian inference. *Ecological Modelling,* 159, 269–277.

Raat, K.J.; Vrugt, J.A.; Bouten, W., and Tietema, A., 2004. Towards reduced uncertainty in catchment nitrogen modelling: quantifying the effect of field observation uncertainty on model calibration. *Hydrology and Earth System Sciences,* 8(4), 751–763.

Refsgaard, J.C. and Storm, B., 1996. Construction, calibration, and validation of hydrologic models. *In*: Abbott, M.B., and Refsgaard, J.C. (eds.), *Distributed Hydrological Modeling.* Water Science and Technology Library, Volume 22. Dordrecht, The Netherlands: Kluwer Academic Publishers, pp. 41–54.

RODRIGUEZ-ITURBE, I. and MEJIA, J., 1974. On the transformation of point rainfall to areal rainfall. *Water Resources Research,* 10, 729–735.
SIMENSTAD, C.; REED, D., and FORD, M., 2006. When is restoration not? Incorporating landscape-scale processes to restore self-sustaining ecosystems in coastal wetland restoration. *Ecological Engineering,* 26, 27–39.
SINGH, V.P. and CHOWDHURY, P.K., 1986. Comparing some methods of estimating mean areal rainfall. *Water Resources Bulletin,* 22, 275–281.
SOLIS, R.S. and POWELL, G.L., 1999. Hydrography, mixing characteristics, and residence times of Gulf of Mexico estuaries. *In:* BIANCHI, T.S., PENNOCK, J.R., and TWILLEY, R.R., (eds.), *Biogeochemistry of Gulf of Mexico Estuaries.* New York: John Wiley and Sons, pp. 29–61.
STONE, G.W.; GRYMES, J.W.; DINGLE, J.R., and PEPPER, D.A., 1997. Overview and significance of hurricanes on the Louisiana coast, USA. *Journal of Coastal Research,* 13, 656–669.
SUMNER, D.M. and BELAINEH, G., 2005. Evaporation, precipitation, and associated salinity changes at a humid, subtropical estuary. *Estuaries* 28(6), 844–855.
SWENSON, E.M. and TURNER, R.E., 1998. Past, present and probable future salinity variations in the Barataria basin system. Prepared for Coastal Restoration and Management. Baton Rouge, Louisiana: Louisiana Department of Natural Resources, 112p.
THOM, R.M., 2000. Adaptive management of coastal ecosystem restoration projects. *Ecological Engineering,* 15, 365–372.
TURNER, R.E, 2006. Will lowering estuarine salinty increase Gulf of Mexico oyster landings? *Estuaries and Coasts,* 29,345–352.
UNCLES, R.J. and PETERSON, D.H., 1996. The long-term salinity field in San Francisco Bay, *Continental Shelf Research,* 16(15), 2005–2039.
VISSER, J.M.; SASSER, C.E.; CHABRECK, R.H., and LINSCOMBE, R.G., 2000. Marsh vegetation types of the Chenier Plain, Louisiana, USA. *Estuaries,* 23, 318–327.
VISSER, J.M.; STEYER, G.D.; SHAFFER, G.P.; HOPPNER, S.S.; HESTER, M.W.; REYES, E.; KEDDY, P.; MENDELSSOHN, I.A.; SASSER, C.E., and SWARZENSKI, C., 2003. Habitat switching module, Chapter 9. *In:* TWILLEY, R.R. (ed.), Coastal Louisiana Ecosystem Assessment and Restoration (CLEAR) Model of Louisiana Coastal Area (LCA) Comprehensive. Ecosystem Restoration Plan. Volume I: Tasks 1–8. Final Report to Department of Natural Resources, Coastal Restoration Division, Baton Rouge, Louisiana. Contract 2511-02-24. 319p.
VRUGT, J.A.; DEKKER, S.C., and BOUTEN, W., 2003. Identification of rainfall interception model parameters from measurements of throughfall and forest canopy storage. *Water Resources Research,* 39(9), 1251, doi:10.1029/2003WR002013.
VRUGT, J.A.; GUPTA, H.V.; BOUTEN, W., and SOROOSHIAN, S., 2003. A Shuffled Complex Evolution Metropolis algorithm for optimization and uncertainty assessment of hydrological model parameters. *Water Resources Research,* 39(8), 1201.
WISEMAN, W.J., JR., and SWENSON, E.M., 1989. Modelling the effects of produced water discharges on estuarine salinity. *In:* BOESCH, D.F., and RABALAIS, N.N (eds.), *Environmental Impact of Produced Water Discharges in Coastal Louisiana.* Chauvin, Louisiana: Louisiana University Marine Consortium, 287p.
WISEMAN, W.J., JR.; SWENSON, E.M., and POWER, J., 1990. Salinity trends in Louisiana estuaries. *Estuaries,* 13(3), 265–271.

APPENDIX

Barataria Mass Balance Model Calculations

To describe the components of the water and salt balance and how each is calculated by the model, the Barataria basin was divided into four subbasins (Figure 2). The surface area of each subbasin (A_t) was partitioned into two parts: water surface area (A_w) and wetland and land surface area (A_l).

Volumes of Subbasins (V)

Volume of water in each subbasin j and for each month i is calculated according to monthly changes in the relative sea level (SL).

$$V_j^i = V_j^{i-1} + (\mathrm{SL}^i - \mathrm{SL}^{i-1})A_{w,j} \tag{A1}$$

Net Supply of Fresh Water (Q_R)

The monthly net supply of fresh water to each subbasin is calculated as in Equation (A2),

$$Q_{R,j}^i = R_j^i A_t - E_j^i A_w - E_c E_j^i A_l + Q_{D,j}^i \tag{A2}$$

where R_j^i, E_j^i and $Q_{D,j}^i$ represent rainfall, potential evaporation, and river diversion, respectively, for subbasin j and month i. The model calculates losses from waterbodies at the potential rate of evaporation, whereas losses from wetland and land areas are calculated as a fraction of the potential rate of evaporation. The fraction E_c is one of the model parameters to be determined through calibration.

Mean Flows among Subbasins (Q_o)

The excess of water volume (N) in each subbasin is calculated first.

$$N_j^i = (V_j^i - V_j^{i-1}) - Q_{R,j}^i \tag{A3}$$

Water excesses are used to calculate mean flow advection fluxes (Q_o) between each connected pair of subbasins. According to the schematic shown in Figure 2, the following fluxes need to be calculated: $Q_{o,1-2}$ between subbasins 1 and 2, $Q_{o,2-3}$ between subbasins 2 and 3, $Q_{o,3-4}$ between subbasins 3 and 4, and $Q_{o,4-G}$ between subbasin 4 and the Gulf of Mexico. In addition, hydraulic connections in the Barataria basin indicated that water can flow between subbasins 2 and 4, which is represented by $Q_{o,2-4}$. The following set of equations is used to solve for each Q_o.

$$\begin{aligned} Q_{o,1-2}^i &= N_1^i, \\ Q_{o,2-3}^i &= N_2^i + Q_{o,1-2}^i - Q_{o,2-4}^i, \\ Q_{o,3-4}^i &= N_3^i + Q_{o,2-3}^i, \\ Q_{o,4-G}^i &= N_4^i + Q_{o,2-4}^i + Q_{o,3-4}^i. \end{aligned} \tag{A4}$$

Water Exchange Fluxes (X)

Exchange fluxes among the different subbasins occur as a result of dispersion and wind and tidal mixing. To understand the exchange flux, consider that at any time during a certain month, the discharge of water between the estuarine basin and the Gulf of Mexico can be represented as a sum of a time-varying component and the (constant) mean discharge for that month Q_o. The exchange flux X (same units as Q_o) represents the average magnitude of the time-varying component of discharge. In the current model formulation, the exchange flux X for each pair of subbasins is a represented as a parameter to be estimated by calibration. Similar to Q_o, there are five of these exchange fluxes (parameters): X_{1-2}, X_{2-3}, X_{2-4}, X_{3-4}, and X_{4-G}. Although the mean discharge Q_o

varies from month to month in response to changes in sea level and in the net supply of fresh water, the model uses the same value of each exchange flux X in its calculation of salinity through the entire period of simulation.

It should be noted that although Equation (A4) includes five unknown Q_o fluxes, continuity provides only four equations for their solution. This situation arises from the additional flux term Q_{2-4}, which was added to represent the connection between subbasins 2 and 4. We addressed this condition by assuming that the relative magnitudes of mean discharge fluxes (Q_o) arranged in parallel are in the same proportion as the corresponding set of exchange fluxes X. Both the mean discharge and the exchange flux arise from an underlying hydraulic connection; therefore, it is reasonable to assume that the pathway with the larger exchange flux would also support the larger mean discharge. This results in an additional relationship between Q_{2-4} and Q_{2-3} [Equation (A5)].

$$Q^i_{o,2-4} = Q^i_{o,2-3} X_{2-4}/X_{2-3} \tag{A5}$$

Advective Fluxes of Salt (SQ)

For each time step, the advective salt fluxes associated with the mean fluxes of water are calculated as the product of Q_o between each two connected subbasins and the salinity S of the "upstream" subbasin. For example, SQ_{1-2} is calculated as $SQ^i_{1-2} = Q^i_{o,1-2} S^i_1$ if the flow direction is from subbasin 1 to subbasin 2, or as $SQ^i_{1-2} = Q^i_{o,1-2} S^i_2$ if the flow is in the opposite direction. Similar calculations are applied for the other advective fluxes SQ_{1-2}, SQ_{2-3}, SQ_{3-4}, and SQ_{2-4}. The flux between the Gulf and subbasin 4, SQ_{4-G}, is similarly calculated with either S_4 or the boundary salinity S_B.

Exchange Fluxes of Salt (SX)

After the flow directions assumed in Figure 2, fluxes of salt carried by exchange flows are calculated as the product of X between each two connected subbasins and the difference in their salinities. For example, SX_{1-2} is calculated as $SX^i_{1-2} = X_{1-2}(S^i_2 - S^i_1)$. Similar calculations are used for the other flux terms SX_{1-2}, SX_{2-3}, SX_{3-4}, SX_{2-4}, and SX_{4-G}.

Subbasin Salinity (S)

Finally, the monthly average salinity in each subbasin is calculated by dividing the salt content by the volume of water in the subbasin. For example, salinity in subbasin 1 is calculated as in Equation (A6).

$$S^{j+1}_1 = \frac{S^j_1 V^j_1 + SQ^j_{1-2} + SX^j_{1-2}}{V^{j+1}_1}. \tag{A6}$$

Similar calculations are performed to estimate monthly salinities in the other three subbasins.